CONF-790611--1

MASTER

LA-UR -78-3169

TITLE: HEAT PIPE THERMAL CONTROL OF SLENDER OPTICS PROBES

AUTHOR(S): F (rancis) C (oyne) Prenger

SUBMITTED TO: To be presented at the AIAA Terrestrial Energy Systems Conference on June 4-6, 1979 in Orlando, Florida.

los alamos
scientific laboratory
of the University of California
LOS ALAMOS, NEW MEXICO 87544

An Affirmative Action/Equal Opportunity Employer

Form No. 836
St. No. 2629
1/75

UNITED STATES
ENERGY RESEARCH AND
DEVELOPMENT ADMINISTRATION
CONTRACT W-7405-ENG. 36

HEAT PIPE THERMAL CONTROL OF SLENDER OPTICS PROBES

F. C. Prenger*

ABSTRACT

The thermal design for a stereographic viewing system is presented. The design incorporates an annular heat pipe and thermal isolation techniques. Test results are compared with design predictions for a prototype configuration. Test data obtained during heat pipe startup showing temperature gradients along the evaporator wall are presented. Correlations relating maximum wall temperature differences to a liquid Reynolds number were obtained at low power levels. These results are compared with Nusselt's Falling Film theory.

INTRODUCTION

A stereographic viewing system to be used in the international reactor safety experiments in Germany (PKL) and Japan (JAERI) utilizes a methanol-filled, annular heat pipe[1,2] as the principal element of its thermal control system. The viewing system or optic probe enables flow visualization of processes internal to a steam-filled pressure vessel with internal temperatures to 300°C. The probes have a maximum diameter of 50 mm and lengths up to 3.4 m. Two 5 mm diameter lenses surrounded by fiber optics are enclosed in a 12 mm o.d. stainless steel tube. The twin lenses are the optical link between the viewing location inside the pressure vessel and the video converter located externally. The fiber optics transmit light to the

*Staff member Los Alamos Scientific Laboratory, Los Alamos, New Mexico

subject from an external light source. At the viewing end of the optics tube are steerable mirrors and lenses for focusing on the subject. This lower cavity is enclosed with viewing accomplished through a sapphire window. The optical elements of the system must be maintained below $150^{o}C$ to prevent structural damage, and temperature gradients along the probe axis must be minimized to provide acceptable image quality.

Because of space limitations in the reactor the maximum probe diameter is 40 mm for PKL and 50 mm for JAERI. The limited cross-sectional area combined with the long length creates a severe thermal control problem i.e., a large external surface area with resulting high heat loads to the probe and limited space for a thermal control device to remove the heat load. A heat pipe is uniquely suited to provide thermal control for this application.

The heat pipe which is annular in cross-section and surrounds the optics tube is vertical with the evaporator at the bottom and operates with gravity-assist. During testing of the heat pipe, excessive temperature differences along the wall associated with the startup were observed. For this reason methanol was chosen as the working fluid. Although water provides more capacity due to a higher latent heat of vaporization, methanol produces lower axial temperature gradients during startup. The thinner liquid film obtained with water appears to inhibit uniform wetting of the wick. Also the use of a graded wick has been found by others[3] to improve wall wetting of the working fluid. For this reason a graded wick was selected for this application. Although the temperature gradients disappeared with increased power their presence is an indication of a minimum performance limit. Data associated with this phenomena are presented and correlations relating the temperature gradients to the power level are proposed.

THERMAL DESIGN

The objective of the thermal design of the probe is to provide an isothermal ent for the optical elements and minimize the heat transfer to the annular pipe thus requiring a minimum vapor passage cross-sectional area. Figure illustrates elements of the thermal control system. The central, 1.43 cm diameter core of the annulus contains the two lens assemblies and fiber optics. Surrounding the core is the annular cavity comprising the heat pipe. The outside diameter of the heat pipe outer wall is 2.5 cm. An outer screen of 100 mesh and an inner screen of 60 mesh comprise the heat pipe wick which is located along the outer wall. A second annular space containing Xenon at one atmosphere ($20^{o}C$) surrounds the heat pipe. The Xe layer provides thermal isolation from the external environment.

The lower end of the probe which contains optical elements for obtaining the desired viewing angle and imaging is structurally tied to the heat pipe providing thermal control via conduction through these attachments. In addition, the lower cavity is also Xe filled providing thermal isolation.

For thermal design purposes the upper end of the probe is divided into three elements. The lower or first element is the mounting structure attaching the probe assembly to the pressure vessel. The mounting structure provides for vertical positioning and rotation of the probe. Incorporated in the mounting structure is a 8.5 cm long collar with a maximum wall thickness of 0.17 cm forming a thermal standoff isolating the pressure vessel from the heat pipe condenser. Above the condenser the heat pipe cavity terminates. Extending beyond the heat pipe in the upper or third section will be video electronics and a light source with a combined power dissipation of 350 W.

The thermal control system objectives are accomplished by combining the high effective thermal conductivity of the heat pipe with thermal isolation techniques.

ISOTHERMAL CONTROL OF THE LENS/FIBER OPTICS

Use of the heat pipe provides for isothermal conditions along the axis of the probe for variable heat loads less than the capacity of the heat pipe. The heat pipe has a 20 cm condenser which is surrounded by a two-pass, annular heat exchanger. Cooling requirements for the condenser are 64 g/s (1.0 GPM) of water at a maximum temperature of 30°C, this allows a maximum temperature change across the liquid layer in the heat pipe condenser of 40°C. The estimated film thickness is 0.015 mm which corresponds to a temperature drop of 2°C which is well below the available ΔT. The hydrodynamic capacity of the heat pipe exceeds 1500 W for the 3.4 m JAERI configuration. The vapor flow area is 2 cm^2 resulting in a vapor flow velocity well below sonic.

THERMAL ISOLATION

The Xe filled cavity, lined with a vacuum deposited gold coating and surrounding the heat pipe, limits the heat transfer through the probe wall to 126 W. Xenon is used as the fill material because of its low thermal conductivity and its stability in the presence of temperature gradients. The Xe also occupies the lower tip of the probe and here the spacing between the probe outside wall and the lens support structure must be kept below 1 cm, the minimum spacing for the onset of convection for the existing conditions. Since thermal control of the lower optics is via conduction through the structure to the lower end of the heat pipe cavity, the support structure is a high thermal conductivity material such as aluminum or copper. If convection were permitted in the lower cavity the heat leak in this area would increase four-fold.

A centering mechanism consisting of stainless steel wire clips welded to the outer wall of the heat pipe is used to maintain alignment of the heat pipe assembly. There are a total of six clips and the total heat gain through these clips is 8 W. A summary of the heat transfer to the heat pipe is shown in Fig. 2 for both the PKL and JAERI configurations.

THERMAL TESTING

A systems test of the optic probe was performed. The central optical tube was instrumented with thermocouples with the axial distribution shown in Fig. 3. Also, viewing windows normally installed in the lower cavity were not available for this test and a dummy cap of stainless steel was substituted. The heat pipe evaporator boundary condition was constant wall temperature which correctly simulates the environment within the PKL reactor.

The test fixture consisted of an insulated, steam-filled pressure vessel (12 cm o.d.). Saturated steam was supplied to the test fixture via a steam generator with a capacity of 45 kg/h at 7.0 ATM pressure. By measuring the vessel pressure and assuming saturated conditions within the test fixture, the environment temperature was determined.

Three tests were run at the maximum pressure of 7.0 ATM (with a corresponding temperature of 167°C). All tests started at ambient temperatures and reached maximum operating temperature in 1 h. This startup is estimated to be at least ten times faster than the startup of the PKL facility, therefore, any tendency of the heat pipe to overheat during startup would be greatly accentuated by this test. No significant overheating occurred.

During the course of the tests data were collected every 5 minutes. These data included the 15 thermocouples located in the optics tube, the steam pressure in the test section, the heat pipe condenser coolant inlet and outlet temperature, and coolant flowrate. The power transmitted by the heat pipe was determined using the condenser cooling water flowrate and the temperature rise of the coolant. At steady-state this power is equal to the heat leak to the probe.

Steady-state temperature profiles for the three runs are shown in Fig. 4. For Runs 1 and 2 the annular space surrounding the heat pipe was filled with Xe at 1.5 ATM. For the third run the Xe was evacuated and the annulus was back-filled with air at atmospheric pressure. Changing from Xe to air increased the heat load on the system from 50 W in Runs 1 and 2 to 120 W for Run 3. Figure 4 shows a change in operating temperature between Runs 1 and 2. This difference is believed caused by an accumulation of non-condensible gas in the heat pipe. Prior to Run 2 the heat pipe was vented momentarily to remove the non-condensible gas which then resulted in the "flat" temperature profile shown for Run 2. Run 3 exhibits a temperature variation of 2.5^{o}C along the length of the evaporator. This results from the higher power carried by the heat pipe during this run. The low wall temperatures near the bottom of the evaporator can be attributed to agitation of the methanol pool and subsequent localized cooling of the walls, whereas the higher temperatures near the condenser result from partial dryout of the wick due to some vaporization of the return liquid below the condenser. The observed temperature gradients are not expected to adversely affect the performance of the optics system.

Figure 4 also shows that the heat pipe operating temperature, defined as the average wall temperature, is weakly related to the heat load and strongly influenced by the coolant inlet temperature. The heat pipe operating temperature is slightly above the coolant inlet temperature regardless of the heat load. The increase in temperature at the evaporator end or bottom of the heat pipe shown in Fig. 4 is caused by the end thermocouple not being attached to the heat pipe wall. Because the optics was not installed for this test, a rubber stopper was used to seal the inner tube at the bottom. The end thermocouple was resting against this stopper.

Figure 5 shows a comparison between the predicted heat load from the thermal analysis and the actual heat load as measured by the heat rejected in the heat pipe condenser. For the Xe filled annulus two predictions are shown, one with free convection in the annulus and one without free convection. However, for air the Grashof Number is lower than for Xe and free convection of the air is not likely to occur. The higher measured heat load probably results from underestimating heat leaks from penetrations across the annular space and in the lower optics cavity.

The test results show that the thermal control system is adequate to maintain temperature differences along the axis of the optics tube below $3^{o}C$. The system is also capable of rejecting the worst-case heat load, i.e., replacement of Xe by air in the annulus while maintaining the same operating temperature. Also, overheating due to rapid startup of the system was not observed. It should also be noted that with a low operating temperature (below $30^{o}C$) quenching of the probe exterior will have little effect on the temperature stability since the heat flow will always be into the probe. The operating temperature will be maintained by a decrease in the power transported by the heat pipe. This temperature stability is especially desirable since the most critical time for data gathering is during and immediately after simulation of the emergency core coolant system operation which involves quenching of the probe exterior.

HEAT PIPE STARTUP PERFORMANCE

In the heat pipe tests temperature gradients along the heat pipe evaporator were observed at low powers and are believed associated with incomplete filling of the wick. The gradients decrease with increasing power until the wicking limit of the heat pipe is approached, whereupon the gradients reappear. The phenomena causing these startup temperature gradients, which represent a lower limit to satisfactory heat pipe performance, is of interest to heat pipe designers.[4] The test data were analyzed to find a correlation which might be useful in predicting the temperature gradients.

Since the startup temperature gradients are inversely related to the power transported by the pipe a Reynolds number based on the liquid properties and the heat pipe diameter was used as the independent variable, or

$$Re_L = \frac{V_L \rho_L D}{\mu_L} \tag{1}$$

Where

V_L is the liquid velocity

ρ_L is the liquid density

D is the heat pipe diameter

μ_L is the liquid viscosity

The temperature gradient along the evaporator was characterized by the maximum temperature difference, ΔT_m. Although this parameter is dependent on the number and distribution of the thermocouples along the heat pipe evaporator, the thermocouple distribution shown in Fig. 3 provides enough information to interpolate between readings when necessary. A dimensionless temperature difference Θ is defined as

$$\Theta = \frac{\Delta T_m K_L}{LH} \tag{2}$$

where

K_L is the liquid thermal conductivity

L is the heat pipe length

H is the liquid transport factor.

The liquid transport factor is referred to in the heat pipe literature[5] and is given by

$$H = \frac{h_{fg} \sigma \rho_L}{\mu_L} \tag{3}$$

where

h_{fg} is the latent heat of vaporization

σ is the surface tension.

The use of σ as the dependent variable introduces the latent heat and surface tension of the working fluid into the correlation. From physical arguments both of these properties are importanc to the startup process. If the temperature gradients are associated with incomplete filling of the heat pipe wick one could describe the process in terms of a balance between surface tension forces tending to bind the liquid into globules and hydrodynamic forces which tend to mechanically distribute the liquid along the wick. In this model of the mechanism the surface tension forces are related to the fluid properties whereas the hydrodynamic forces are related to the heat transport parameters.

Figure 6 shows the dimensionless temperature difference Θ plotted versus the liquid Reynolds number, Re_L. Two working fluids were used, water and methanol. Correlations for each working fluid were obtained using a least squares fit of the test data. For water

$$\Theta = 8.00 \times 10^{-16} Re_L^{-0.309} \qquad (4)$$

and for methanol

$$\Theta = 1.15 \times 10^{-15} Re_L^{-0.45} \qquad (5)$$

To account for the difference in working fluids the Prandtl number was introduced. Figure 7 shows a plot of $\Theta/Re_L^{-0.383}$ versus Prandtl number and again using a least squares fit of the data gives

$$\Theta/Re_L^{-0.383} = 3.25 \times 10^{-16} \, Pr \qquad (6a)$$

or

$$\Theta = 3.25 \times 10^{-16} \, Re_L^{-0.383} Pr. \qquad (6b)$$

The exponent of the Reynolds number (-0.383) was chosen as the average of the slopes of the correlations in Fig. 6. However, the interesting result here is the linear dependence on Prandtl number.

The dimensionless temperature difference Θ can be related to the thickness of the liquid in the wick. Neglecting the wick in a first approximation and using Nusselt's film condensation theory[6] the dimensionless film thickness is related to the liquid Reynolds number by

$$\delta^* = 0.909\ Re_L^{0.333} \tag{7}$$

where

$$\delta^* = \frac{\delta \left[g\ (\rho_L - \rho_v)\ \rho_L \right]^{0.333}}{\mu_L^{0.667}} \tag{8}$$

and

δ is the film thickness

g is the gravitational acceleration

ρ_L is the liquid density

ρ_v is the vapor density.

If the Reynolds number exponent in Eq. (6) is approximated by the one-third power then combining Eq. (6) and (7) gives

$$\Theta = 2.95 \times 10^{-16}\ \frac{Pr}{\delta^*}\ . \tag{9}$$

Equation (9) relates the maximum temperature difference in the evaporator to the inverse of the liquid film thickness and the Prandtl number, a surprisingly simple result.

CONCLUSIONS

The thermal control of a stereographic viewing system is successfully accomplished by using an annular heat pipe in combination with thermal isolation techniques. The thermal design provides nearly isothermal conditions along the optical axis and lens operating temperatures a few degrees above the condenser coolant inlet temperature. Tests of a prototype system have demonstrated these results.

Testing of the prototype heat pipe showed axial temperature gradients in the evaporator at low power levels. These temperature gradients are characterized by a maximum temperature difference and are correlated using a liquid Reynolds number and the Prandtl number of the working fluid. The correlation is given by Eq. (6). In addition by using Nusselt's film condensation theory it can be shown that the maximum temperature difference is proportional to the Prandtl number and inversely proportional to the liquid film thickness, Eq. (9). Although not studied in this investigation, other wick configurations may have a significant influence on axial temperature gradients during heat pipe startup. These effects should be investigated

ACKNOWLEDGEMENTS

The work reported on herein was conducted as reactor safety research for the Nuclear Regulatory Commission under the auspices of the Department of Energy.

REFERENCES:

1. G. M. Grover, T. P. Cotter and G. F. Erickson, "Structures of Very High Thermal Conductances," J. Appl. Phys. V. 35 p. 1990, 1964.

2. T. P. Cotter, "Theory of Heat Pipes," Los Alamos Scientific Laboratory report LA-3246-MS, 1965.

3. C. A. Busse and J. E. Kemme," The Dry-Out Limits of Gravity-Assist Heat Pipes with Capillary Flow," 3rd International Heat Pipe Conf., Palo Alto, CA., 1978.

4. J. E. Kemme, "Heat Pipe Design Considerations," Los Alamos Scientific Laboratory report LA-4221-MS, 1969.

5. P. D. Dunn and D. A. Reay, <u>Heat Pipes</u>, Pergamon Press, Oxford, England, 1976.

6. W. Nusselt, S. ver. deut. Ing., V60, 1916.

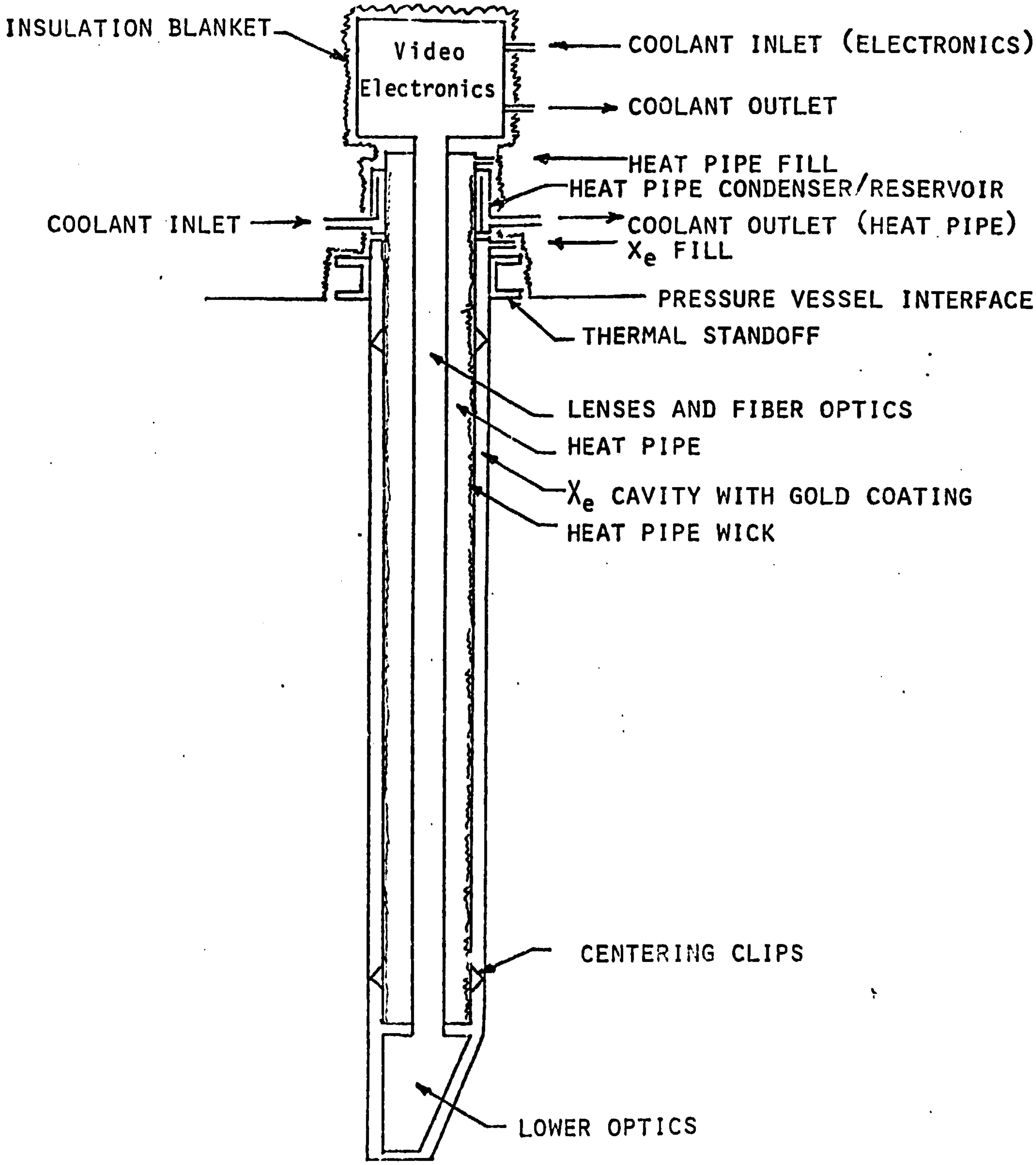

FIG. 1. SCHEMATIC SHOWING THERMAL CONTROL SYSTEM.

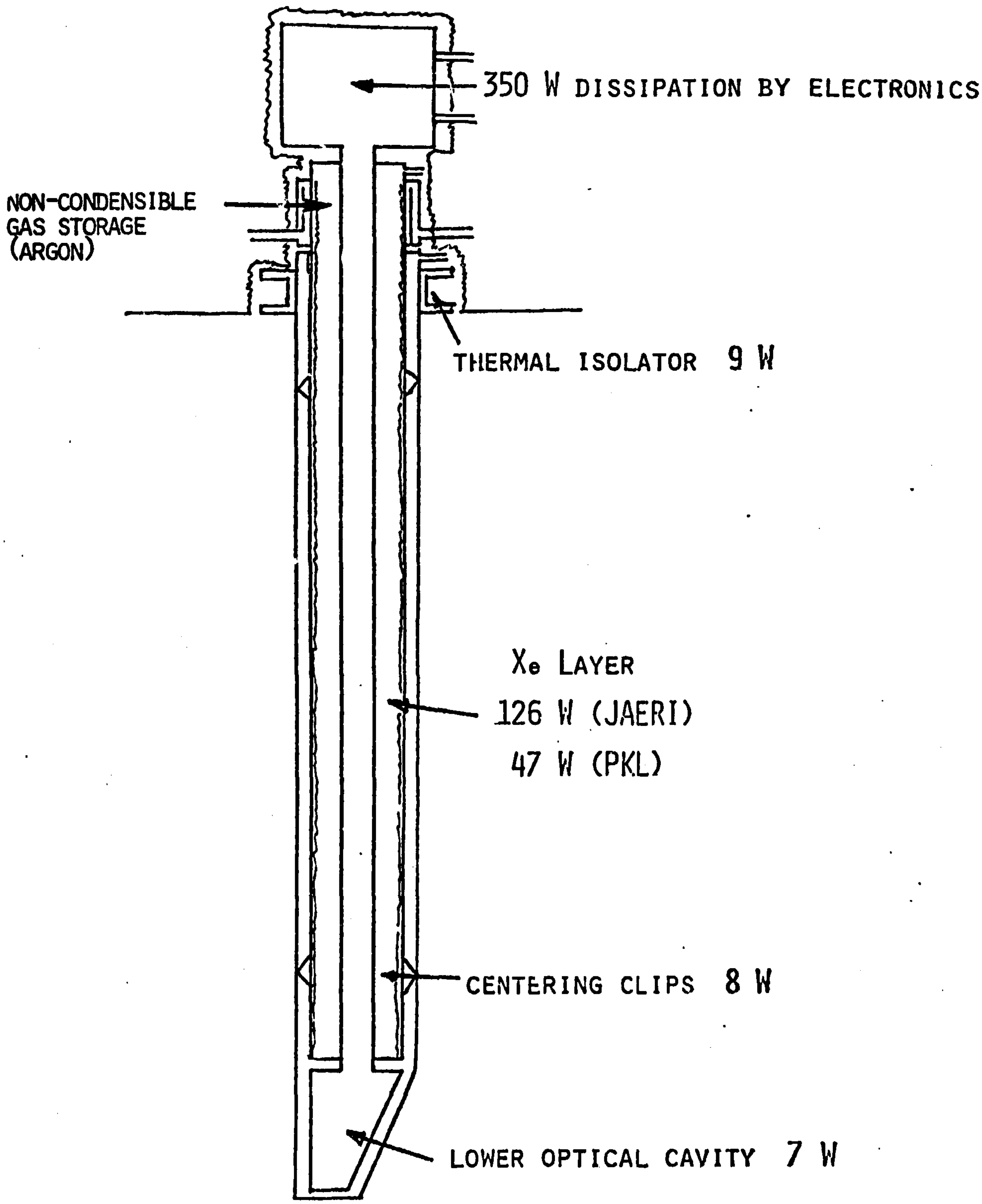

TOTAL HEAT LOAD = 150 W (JAERI)
= 71 W (PKL)

FIG. 2. ENERGY DISTRIBUTION FOR PKL AND JAERI CONFIGURATIONS.

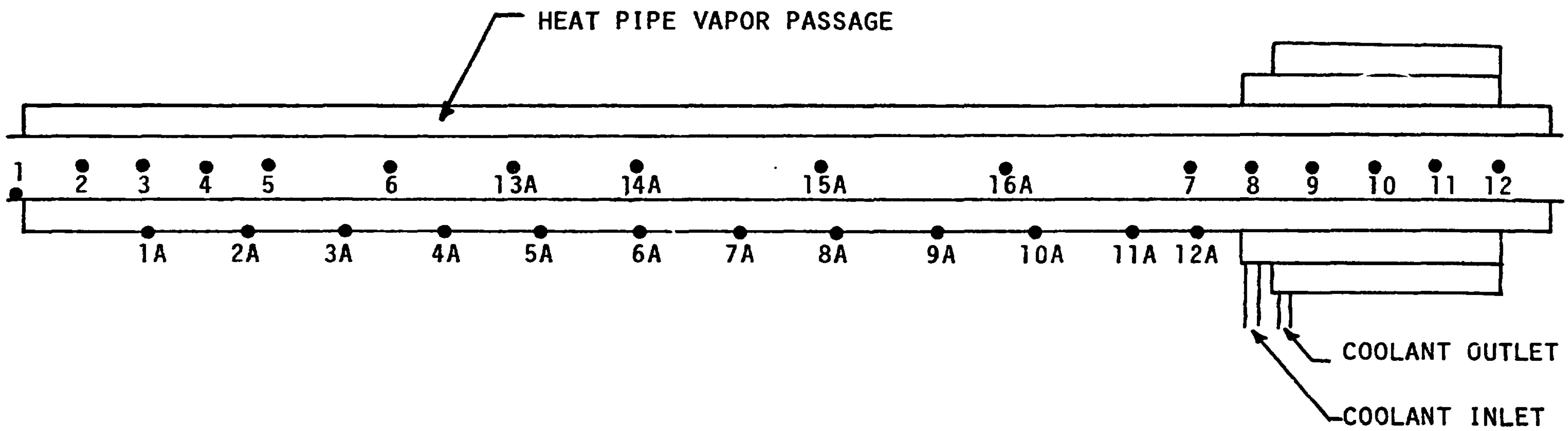

Fig. 3. Prototype heat pipe showing thermocouple locations.

PERFORMANCE OF PKL STEREOGRAPHIC LENS SYSTEM

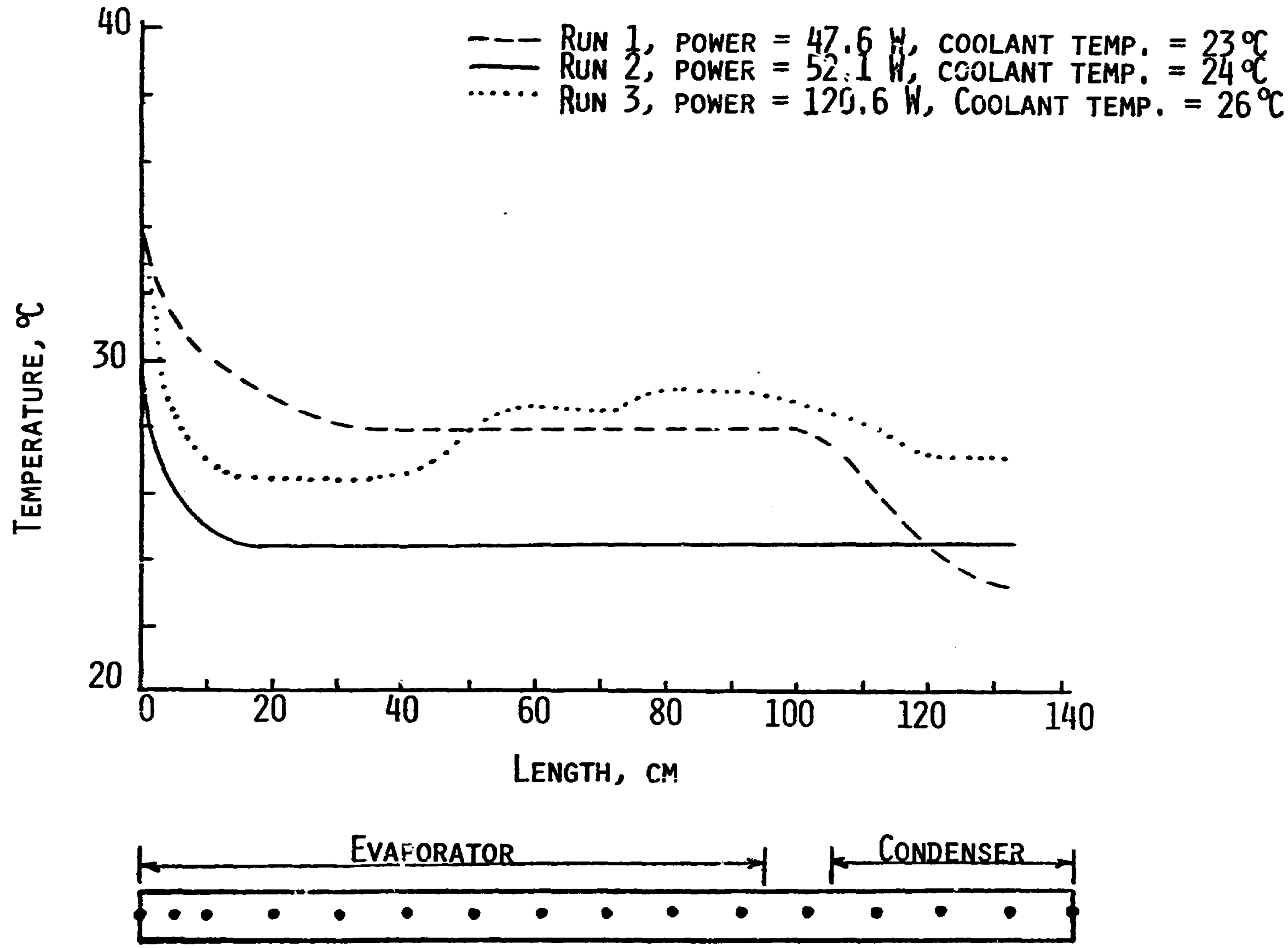

Fig. 4. Steady State Temperature Profiles with 167°C Environment.

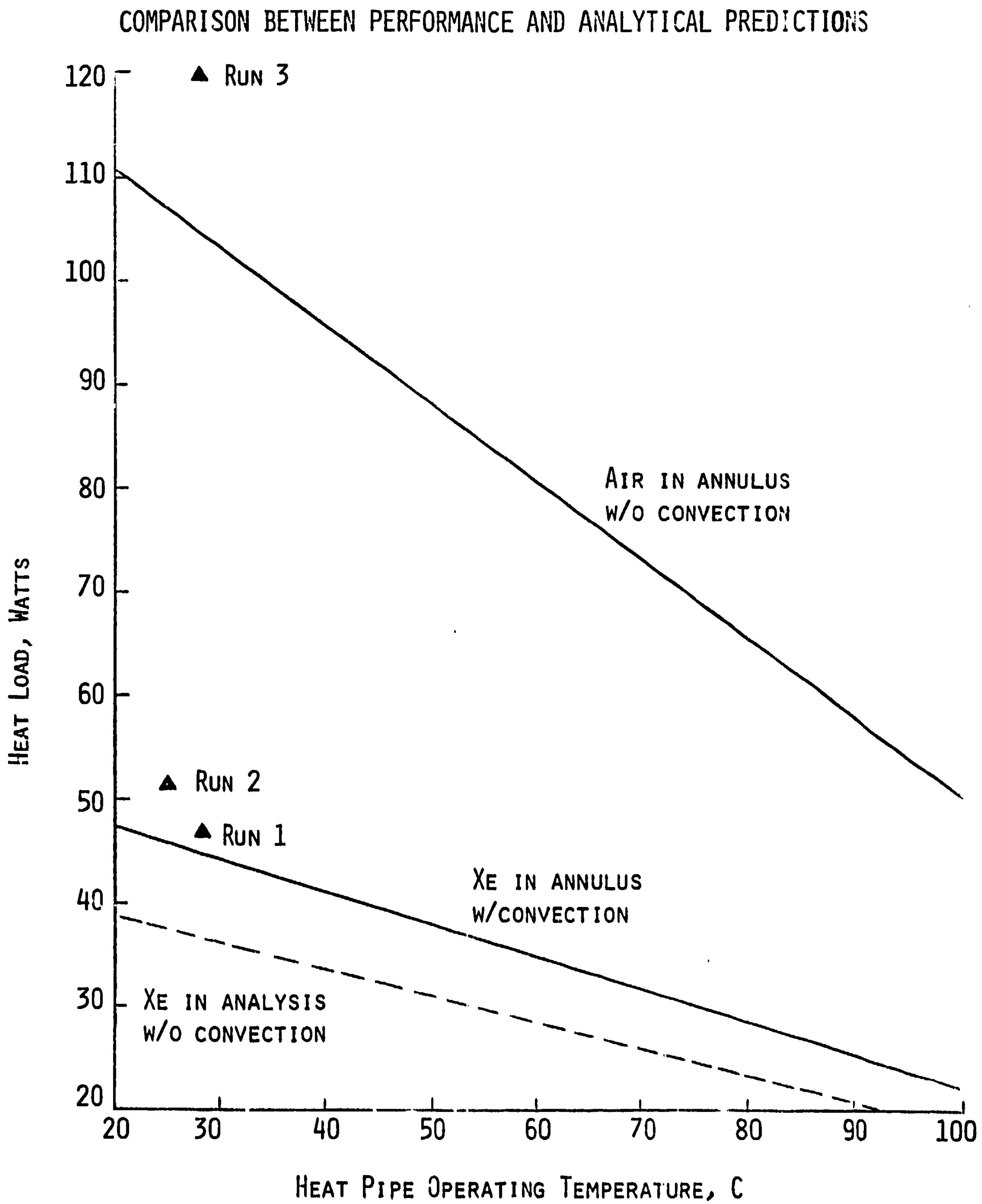

Fig. 5. Comparison Between Performance And Analytical Predictions.

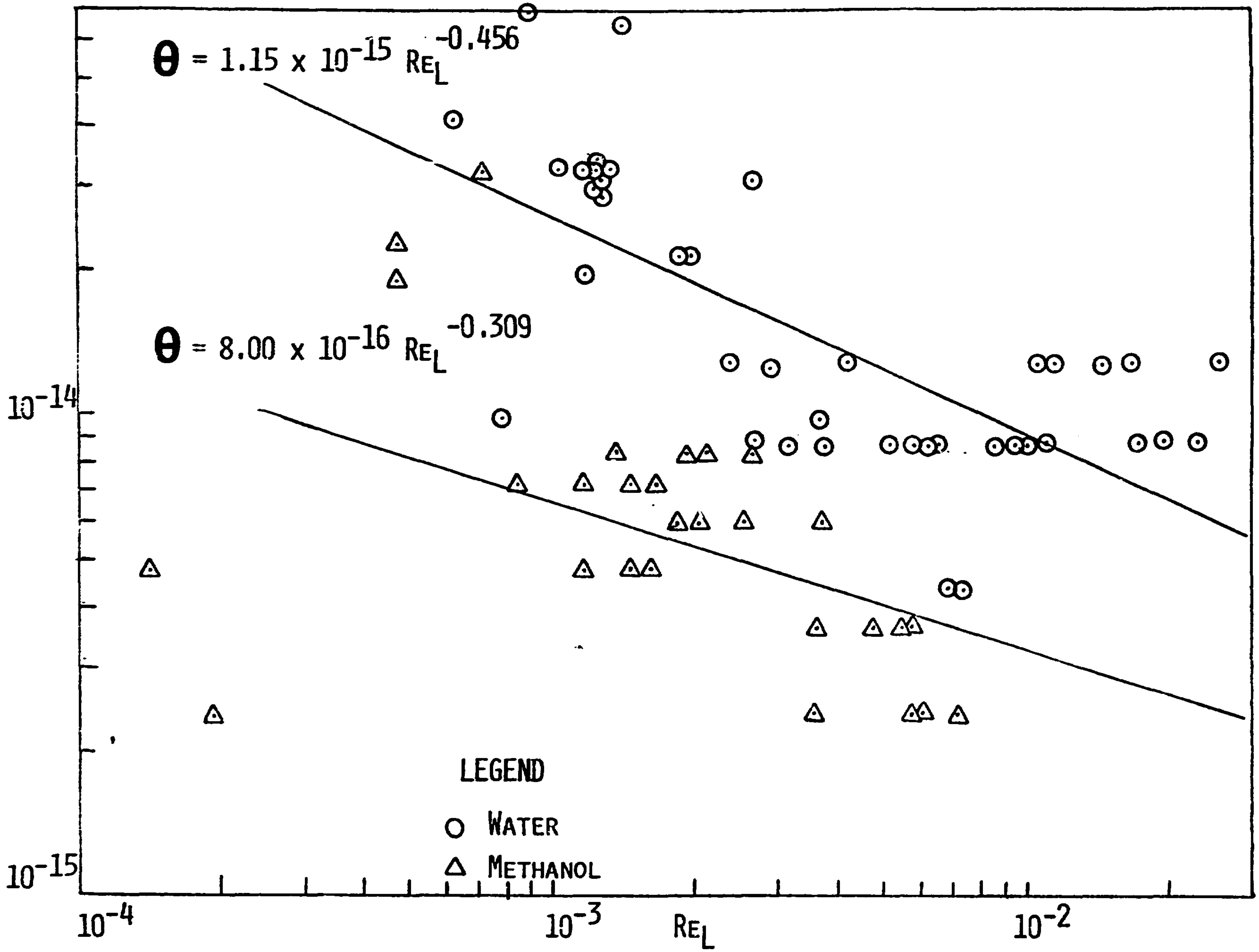

Fig. 6. Dependence of Dimensionless Temperature on Reynolds Number.

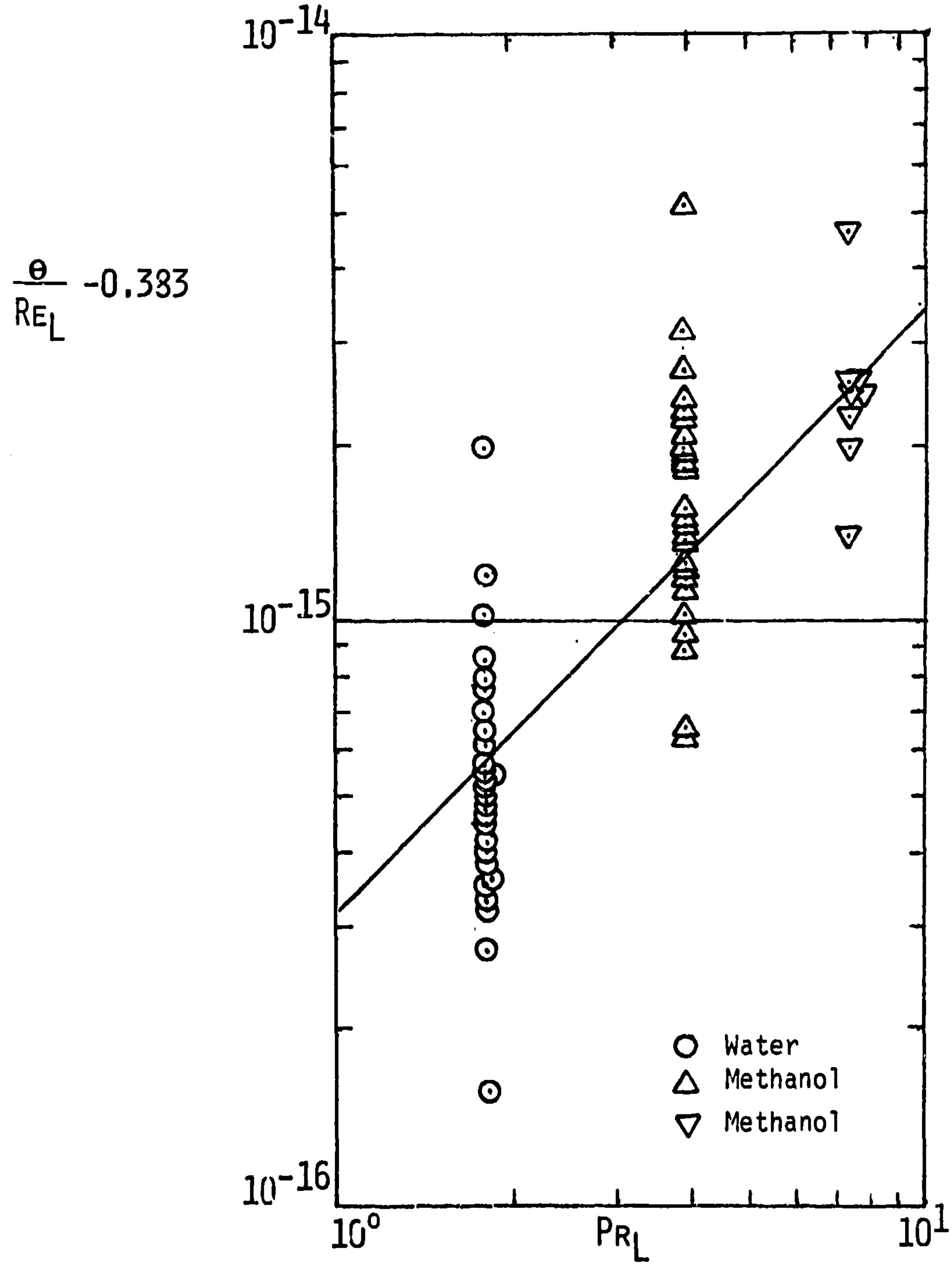

Fig. 7. Dependence of Dimensionless Temperatures on Prandtl Number.